Biogeochemistry (2012) 108:109–118
DOI 10.1007/s10533-011-9576-0

pH change induces shifts in the size and light absorption of dissolved organic matter

Michael L. Pace · Isabel Reche · Jonathan J. Cole · Antonio Fernández-Barbero · Ignacio P. Mazuecos · Yves T. Prairie

Received: 26 August 2010 / Accepted: 25 January 2011 / Published online: 11 February 2011

Abstract Dissolved organic matter (DOM) influences inland water ecosystems through its light absorbing qualities. We investigated how pH affects light absorption by DOM with pH manipulation experiments and with data from two lake surveys. We hypothesized that: (1) light absorption and photobleaching of DOM would increase with increasing pH, and (2) as a result of photobleaching, molar absorption (i.e. light absorbance at 440 nm/dissolved organic carbon concentration) would decrease among lakes with increasing pH. In experiments with filtered lake water both initial light absorption and photobleaching rates increased at higher (i.e. more basic) pH along with a concomitant shift in the size of DOM toward larger colloidal materials measured by dynamic light scattering (DLS). Both scanning electron microscopy (SEM) and atom force microscopy (AFM) revealed large colloidal to particulate-sized organic matter in alkaline relative to acidic treatments. In the lake surveys, molar absorption coefficients were negatively related to pH across gradients similar to the experiments. Our results are consistent with a conceptual model in which at low pH DOM polymers and colloids are condensed limiting exposure of chromophores to light; at higher pH, polymers and colloids are expanded exposing chromophores to light resulting in greater initial light absorption and faster photobleaching. Hence, water transparency, which is significantly controlled by DOM, is sensitive to environmental changes that influence the pH and chemical composition of inland waters.

Keywords Dissolved organic matter · Light absorption · pH · Lakes · Photobleaching · Colloids · CDOM

M. L. Pace (✉)
Department of Environmental Sciences, University of Virginia, 291 McCormick Road, P.O. Box 400123, Charlottesville, VA 22904, USA
e-mail: pacem@virginia.edu

I. Reche · I. P. Mazuecos
Departamento de Ecologia, Universidad de Granada, Granada, Spain

J. J. Cole
Cary Institute of Ecosystem Studies, Millbrook, NY, USA

A. Fernández-Barbero · I. P. Mazuecos
Departamento de Fisica Aplicada, Universidad de Almeria, Almeria, Spain

Y. T. Prairie
Département des Sciences Biologiques, Université du Québec à Montréal, Montreal, QC, Canada

Introduction

Dissolved organic matter (DOM) is a heterogeneous pool of compounds that collectively influences many physical, chemical and biological properties of inland waters (Williamson et al. 1999; Wetzel 2001; Prairie 2008). The concentration of dissolved organic carbon

(DOC) in inland waters depends on inputs from in situ production, uplands and wetlands and from losses due to photo- and bacterial degradation as well as flocculation and sinking (Molot and Dillon 1997; Morris and Hargreaves 1997; McKnight et al. 2001; Von Wachenfeldt and Tranvik 2008; de Vincente et al. 2009). Recent studies indicate that the concentration of DOC regulates productivity in nutrient-poor lakes through light attenuation that limits benthic primary and secondary production (Karlsson et al. 2009). In addition, large-scale environmental trends such as recovery from acidification, climate warming, and land use conversion are altering the concentrations and chemical composition of DOC in streams, rivers, and lakes (De Wit et al. 2007; Monteith et al. 2007; Wilson and Xenopoulos 2009). The effects of these environmental changes on the light absorption properties of DOM, however, are poorly understood. High concentrations of light-absorbing DOM (termed chromophoric DOM or CDOM) reduce transmission of UV and visible light while low CDOM concentrations are associated with clear water and high light transmission (Kirk 1994; Morris et al. 1995).

In prior measurements from 30 lakes we found a strong positive correlation between the rate of photobleaching (i.e. the loss of light absorption with light exposure) and acid neutralizing capacity (Reche et al. 1999). A similar relationship is found using the same data set with pH. However, piecewise regression improves the fit and indicates that there is little change in photobleaching with pH across a range of acidic system and then an increase in photobleaching above a pH of 6.3 (Fig. 1). We hypothesized that the relationship observed for lakes with varying pH was related to the structure of DOM molecules as influenced by hydrogen ion and cation concentrations. This hypothesis was derived both from our comparative lake observations and prior studies of marine DOM and humic materials in soil and water that indicate DOM undergoes structural changes linked to solvent pH and cation concentrations (Santschi et al. 1998; Chin et al. 1998; Mynemi et al. 1999; Baalousha et al. 2006). Specifically, Chin et al. (1998) documented expansion of marine DOM polymer-gels across a pH gradient with an abrupt transition to larger size around a pH of 6. Similarly, humic materials undergo changes in macromolecular structure associated with pH, ionic strength and complexing cations of the solvent (Mynemi et al. 1999; Baalousha et al. 2006). Based on these studies and our results with lakes, we hypothesized that experimentally increasing pH, especially above pH 6–6.5 would cause greater initial light absorption per mole of DOC followed by increased rates of photobleaching. We also hypothesized that the ratio of light absorption per mole of DOC would vary among lakes with otherwise similar chemistry in relation to pH.

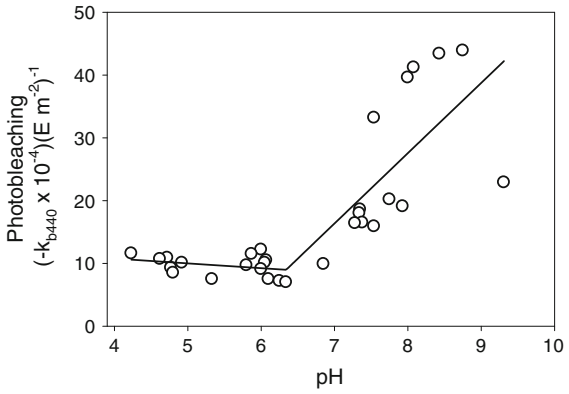

Fig. 1 Relationship between lake pH and photobleaching (loss of absorption) at 440 nm. Data derived from Reche et al. (1999) for lakes ($n = 30$) in Wisconsin, Michigan, New York, and Connecticut (USA). Piecewise regression provides a better fit to the data than a simple linear regression

Here, we present pH manipulation experiments of lake water that document changes in both photochemical properties and colloidal size of DOM with increasing pH. These changes reflect conformational transitions from condensed to expanded phases that result in increasing exposure of chromophores to light. We also provide evidence from multiple lakes that light absorption per mole of DOC is related to pH, consistent with increased light exposure of chromophores at higher pH.

Methods

Experimental manipulations of pH

We used Hummingbird Lake (46°13′N, 89°32′W) located at the University of Notre Dame Environmental Research Center in Michigan (USA) as a source of water for three pH manipulation experiments. Hummingbird Lake is a small (0.8 ha), acidic (average pH = 5.2) system with high concentrations of DOC (average = 1.8 mM C L^{-1}) (Pace and Cole

2002). Water from Hummingbird Lake was filtered through 0.2 μm-filters to remove particles and microorganisms. This filtration minimizes bacterial influence for at least 3–5 days (Reche et al. 1998). We established treatments by adding $NaHCO_3$ to the filtered lake water to create a range of pH values from near 5 to >8. pH treatments (including the nominal pH) were incubated under natural sunlight in Granada (37°8′N, 3°37′W). Subsamples were taken from all pH treatments to establish initial conditions and then incubations were conducted in 37 ml quartz bottles for 47 h. These bottles were spherical flasks with a mean path length (L) of 2.82 cm. At each of 4 time points subsequent to t = 0, three transparent bottles and one dark bottle were removed from sunlight exposure for each pH treatment. The time course of the decay kinetics of absorption coefficients (see below) vs. absorbed sunlight doses was determined for transparent bottles. Dark controls included in the experiment revealed no changes in absorbance over time. The measurement of ambient absorption kinetics across the UV and visible spectrum requires exacting protocols which include optically-thin incubations, control of light spectral composition, and modelling of spectral effects (Miller 1998; Osborne et al. 2001; Del Vecchio and Blough 2002; Tzortziou et al. 2007). In this study, we were interested in relative changes in absorption kinetics as affected by pH and so the procedure we used was adequate for this purpose but less involved than methods needed to model photobleaching as a function of spectral quality, irradiation, and other environmental factors.

All three experiments employed a similar set-up for measuring photobleaching as described next. The experiments differed in whether we made structural observations of DOM and in the techniques employed. No DOM structural observations were made in the first experiment. We used dynamic light scattering (DLS) in the second experiment on all treatments. We also made a few observations using scanning electron microscopy (SEM). In the third experiment we restricted the treatments to high and low pH (described below) and used DLS, SEM, and atomic force microscopy (AFM) to characterize structural aspects of the DOM.

At the beginning and end of the experiment water samples for DOC analysis were filtered through GF/F filters. Samples were subsequently acidified and bubbled prior to analysis by high temperature combustion with a Shimadzu TOC-5050 Analyzer. The method provides a measure of the non-purgeable organic carbon fraction (Findlay et al. 2010). Absorbance scans from 300 to 700 nm were conducted on water samples taken at each time point during the experiments using a 10 cm quartz cuvette in a Perkin-Elmer Lambda 40 spectrophotometer. Internal backscattering was corrected by subtracting the absorbance at 700 nm (Bricaud et al. 1981). Absorbance was expressed as absorption coefficients (Miller 1998) in units of m^{-1} at the specific wavelength of 440 nm (a_{440}). This wavelength was selected to compare with previous studies (Reche et al. 1999) and because CDOM in freshwaters is usually expressed at this wavelength (Cuthbert and del Giorgio 1992). Molar absorption coefficients were obtained by dividing a_{440} values by DOC concentration in mM C L^{-1}. Photobleaching coefficients (k_{b440}) were experimentally calculated from decay kinetics of absorption coefficients of lake water exposed to sunlight. The photobleaching coefficient is the slope of the log-linear regression between the absorption coefficients at 440 nm and absorbed cumulative sunlight doses during incubations of experimental bottles.

Photobleaching coefficients (k_b) were calculated using the equation:

$$a_n = a_0 e_b^{-k} E_a \quad (1)$$

where a_0 (m^{-1}) is the initial absorption coefficient and a_n (m^{-1}) is the absorption coefficient (m^{-1}) at individual sampling times during the incubation, all measured at $\lambda = 440$ nm. Ea (E m^{-3}) is the absorbed dose of sunlight energy at $\lambda = 440$ nm obtained using the equation of Miller (1998):

$$E_a = E_0\left(1 - 10^{a/2.203L}\right) S/V \quad (2)$$

where E_0 is incident sunlight dose at 440 nm (E m^{-2}) that was monitored with a portable spectroradiometer (LiCor Model LI-1800), L (m) is the mean path length of the quartz bottles (2.828 cm), S is surface area (m^2) of a collimated light beam passing through the sample, and V is the volume (m^3) of solution that was exposed to sunlight. Note we should technically include the wavelength (440 nm) in the notations for the absorption coefficient (a_n, a_0) and for the incident sunlight doses (E_a) in Eqs. 1 and 2 as each parameter is wavelength specific (e.g. $a_n = a_{n440}$). However for

ease in notation and clarity, we have excluded specifying the wavelength in Eqs. 1 and 2. Further details on photobleaching rate calculations can be found elsewhere (Reche et al. 2001).

DOM imaging

Dynamic light scattering (DLS), scanning electron microscopy (SEM), and atomic force microscopy (AFM) were used to make observations on changes in DOM structure during the pH manipulation experiments. These systems provide observations on the abundance and size of DOM molecules in the colloidal to small particulate (1 to >1000 nm) range—the latter due to transformation and assembly that may have occurred during incubations (Verdugo et al. 2004). Colloidal particle size was measured using DLS (Chin et al. 1998). Samples were shaken and 5 ml aliquots were poured directly into the scattering cell positioned in the goniometer of a Malvern 4700 laser spectrometer (Malvern Instruments) equipped with a 632.8 nm wavelength He–N laser with the scattering angle set to 45°. Temperate was controlled at 20° using both a Peltier cell and external bath that helped regulate temperature of the cell. The particle size distribution was calculated from the scattered intensities autocorrelation function using cumulant analysis (Koppel 1972; Frisken 2001). We present the means of these distributions referred to as the hydrodynamic diameter which is the apparent average size of the collection of dynamic, hydrated particles in the solution (Chin et al. 1998). Calibration of the DLS spectrometer was conducted using standard suspensions of monodisperse latex microspheres, 220 ± 6 nm (Duke Scientific Corp.).

For SEM images, one drop of lake water was placed on a glass slide and air dried at room temperature in enclosed petri dishes before imaging (thereby minimizing any perturbation due to dehydration). Samples were rinsed with milliQ water for at least 10 s to minimize formation of artifacts (e.g. salts). After sample preparation, SEM images were taken using a Hitachi S-3500 N system equipped with an energy dispersive X-ray analyzer for elemental microanalysis (Oxford Instruments, model INCA-SIGHT). An operating voltage of 20 kV and a variable pressure mode (20–60 Pa) were employed to observe back-scattering electrons from non-conductive samples that were not covered with conductive material.

For AFM images, sample preparation was identical to that for SEM. AFM images were obtained using an Innova Scanning Probe Microscope (Vecco Instruments). Images were taken in contact mode using a tip (model CONT20A-CP, 10 Ohm phosphorus-doped silicon) attached to the end of a cantilever with a low spring constant (0.9 N m^{-1}). Variations in the interactive forces between the tip and surface (the tip is in permanent contact with the sample) result in a topography-based deflection of the cantilever that is recorded by a photodiode. The image resolution was 512 × 512. Images were analyzed and transformed into three dimensional plots with the software SPM Lab Analysis (Vecco Instruments).

Comparative lake surveys

We conducted two lake surveys measuring a number of common variables in each. We measured DOC, *a440*, and pH for lakes in the vicinity of Hummingbird Lake (northern Michigan, USA) four times monthly from May through August over 8 years (study sites and methods described in Pace and Cole 2002). We calculated the average DOC, *a440*, and pH for each year creating a data set of 165 lake-years. In the second survey, lakes were usually sampled four times (range 2–5) during the summer season in the Eastern Townships of Quebec (Canada) over 3 years creating a data set of 62 lake years (study site and methods described in Carignan et al. 2007). The same parameters, DOC, *a440*, and pH, were measured. We used regression analysis to test for a negative relationship between pH and molar absorption coefficients (i.e. the ratio of *a440* to DOC). Data from the two surveys were also combined and molar absorption coefficients were sorted by pH units. The average and standard deviation were calculated for each pH group. Differences among groups were tested by ANOVA and post-hoc means tests.

Results

pH manipulations

In the first experiment to test rates of photobleaching in relation to pH, there was an increase in initial absorption (before exposure) of light at 440 nm (*a440*) that was positively related to the pH of the

treatments across a thousand-fold gradient in hydrogen ion concentration ($r^2 = 0.90$, $p < 0.01$; Table 1). Exposure to sunlight resulted in photobleaching (i.e. loss of absorbance) in all treatments. Declines in absorption varied from about 30% for acidic conditions to >60% in the most alkaline treatments (Table 1) consistent with the patterns in Fig. 1. Photobleaching rates increased significantly with increasing pH ($r^2 = 0.60$, $p < 0.05$; Table 1). Losses of DOC likely due to photomineralization were modest in all cases (<10%), and final DOC concentrations were not significantly different among treatments (Table 1).

In the second experiment where photobleaching was measured as well as structural attributes of the DOM, there was a similar initial increase in the absorption of light at 440 nm (*a440*) (Fig. 2a) as observed in the first experiment. Absorption was much higher for pHs in the range of 7.9–8.2 (Fig. 2a). Using dynamic light scattering (DLS), we measured the average size of DOM in the colloidal to particulate range. The hydrodynamic diameter of colloidal to particulate-sized DOM was positively related to pH (Fig. 2b). Hydrodynamic diameters were largest for pH treatments in the range of 7.9–8.2 (Fig. 2b) similar to the measures of the initial absorption coefficients (Fig. 2a). The DLS results were consistent with our hypothesized pH-related transitions. Scanning electron microscopy (SEM) revealed the presence of hydrated colloids in the most alkaline pH treatment in the experiment depicted in Fig. 2 (results not shown).

Because we had only limited observations with SEM in the second experiment, we performed a third experiment with two pH treatments of 5.59 and 8.22 adding observations with atomic force microscopy (AFM) in addition to DLS and SEM to further analyze the organic materials in solution. As in the second experiment, larger hydrodynamic diameters were observed with DLS in the alkaline relative to the acid treatment (mean size ± 1 SD: pH 5.59 = 797 ± 617 nm; pH 8.22 = 6924 ± 3233 nm). Striking differences were also found between the two pH treatments in the colloidal to particulate materials visualized with SEM and AFM. SEM for the low pH treatment revealed only small, rounded materials (Fig. 3a) while SEM for the high pH treatment had larger plaque-like material (Fig. 3b). Using AFM, we observed some peaks (near 10 and between 15 and 20 microns on the *x*-axis of the image) as illustrated in the three dimensional scan (Fig. 4a) for the low pH treatment, but these peaks were not well developed. In contrast in the high pH treatment, we observed two well defined peaks of particulate-size material that were approximately 1–3 and 15–20 μm in the horizontal dimension (*x*-axis of the image, Fig. 4b). These materials were much more distinct than in the low pH treatment (note differences in the scales of the *z*-axes in Fig. 4). Overall, the formation of larger colloidal to particulate-like material was much greater at high pH than at low pH.

Lake surveys

Our experimental results predict that for a given level of DOC, water will be most transparent in those lakes with high pH and least in those with low pH. We

Table 1 Changes in absorption coefficients at 440 nm (a_{440}), photobleaching coefficients (k_b), and dissolved organic carbon concentrations (DOC) of lake water exposed to sunlight in relation to an experimental pH gradient. pH measured after $NaHCO_3$ additions to establish the different treatments. Percent loss of initial a_{440} and DOC based of measurements at the beginning (initial) and end (final) of the experiment. Values for a_{440}, photobleaching, and DOC are the means and standard errors of three replicates for each pH treatment

pH	Initial a_{440} (m^{-1})	Final a_{440} (m^{-1})	Loss *a440* (%)	$k_b \times 10^{-3}$ $(E\ m^{-3})^{-1}$	Initial DOC (mM)	Final DOC (mM)	Loss DOC (%)
5.24	20.6 ± 0.2	13.8 ± 0.3	33	5.24 ± 0.38	1.80 ± 0.05	1.81 ± 0.02	0
6.06	21.9 ± 0.2	16.1 ± 0.0	27	3.07 ± 0.15	1.89 ± 0.00	1.77 ± 0.00	6.6
6.46	22.3 ± 0.1	15.0 ± 0.3	33	3.60 ± 0.11	1.94 ± 0.03	1.75 ± 0.04	9.9
7.21	23.6 ± 0.1	13.8 ± 0.5	42	5.23 ± 0.24	1.97 ± 0.02	1.81 ± 0.00	8.1
7.71	24.5 ± 0.1	11.5 ± 0.1	53	8.37 ± 0.48	1.91 ± 0.05	1.81 ± 0.00	5.6
7.92	24.7 ± 0.0	8.8 ± 0.1	64	10.10 ± 0.48	1.92 ± 0.01	1.79 ± 0.03	8.3
8.08	27.0 ± 0.3	9.1 ± 0.5	66	13.48 ± 0.79	1.93 ± 0.00	1.84 ± 0.01	4.2

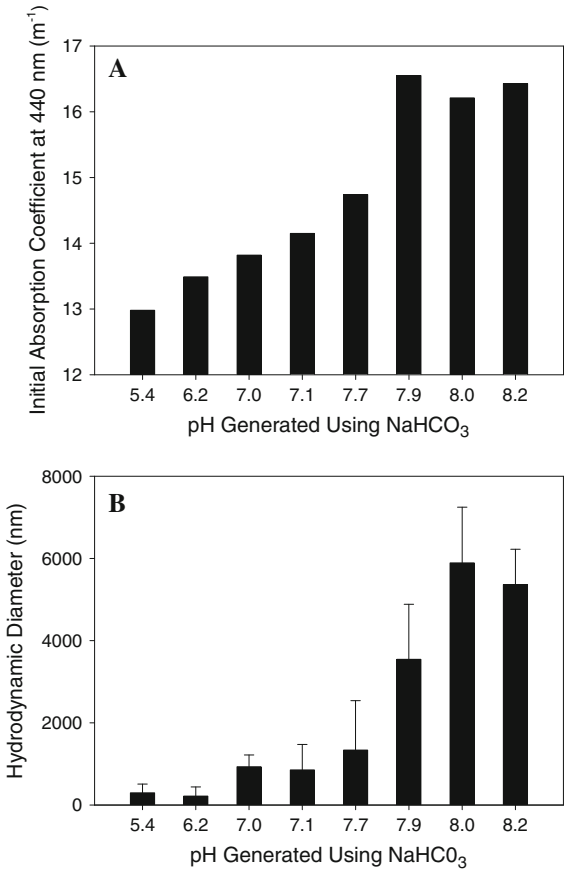

Fig. 2 Changes in (**a**) initial absorption coefficients and (**b**) hydrodynamic diameter of organic matter in pH treatments generated by $NaHCO_3$ additions to lake water. Changes are consistent with a transition of organic matter complexes from condensed (acid pH) to expanded (alkaline pH). Hydrodynamic diameters are means ± standard errors

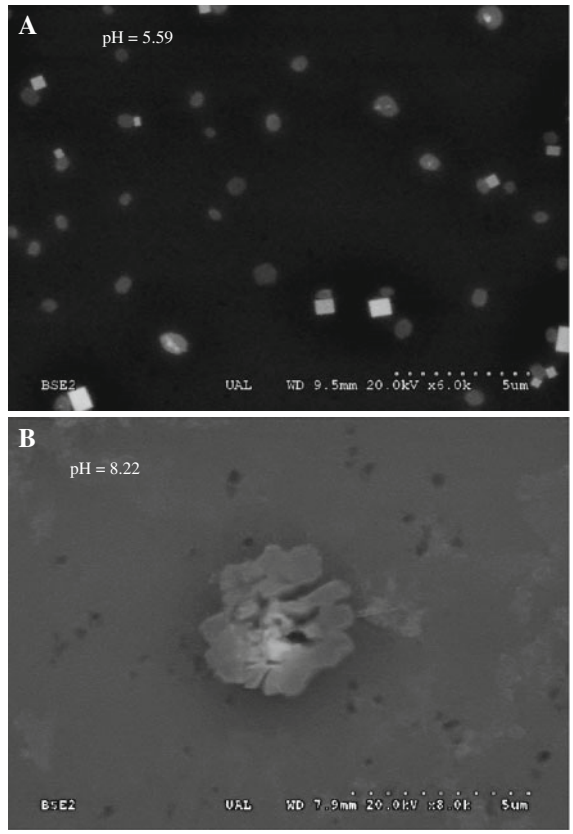

Fig. 3 Scanning electron microscopy images taken of filtered lake water at (**a**) acid and (**b**) alkaline pH. Note the large materials in the pH = 8.22 treatment. Similar structures but with a smaller size were present in the pH = 5.59 treatment. The bright white squares are salt crystals produced when the sample is dried

observed this pattern for the two lake surveys. For either the individual surveys or the combined data, there was a significant ($p < 0.01$) negative relationship between pH and the molar absorption coefficients of DOM (i.e. the ratio of a_{440} to DOC). However, the relationship with pH alone explains only part of the variance in molar absorption (r^2 values <0.27). Other factors independent of pH including the origin of DOM, light-exposure, and iron concentrations are likely important regulators of this ratio (e.g. Reche et al. 2001; Kelton et al. 2007).

Organizing the data into pH categories illustrates the overall pattern (Fig. 5) and allowed us to test for differences among groups. ANOVA was highly significant ($p < 0.0001$) and a post-hoc means test identified three groups. Molar absorption coefficients were highest in lakes with pHs <5 and lowest for groups with pH >7. There was a third, intermediate group of lakes in the pH 5–7 range, but the low (acidic) end of this group (pH group 5–6) overlapped with the most acidic lakes (Fig. 4).

Discussion

The experimental changes in the initial optical properties and mean size of DOM in relation to pH appear to depend on solvent ionic conditions that promote structural changes in DOM molecules. However over the course of exposure to light in both our experiments and in natural systems, it is also possible that changes in DOM molecules might result from selective losses due to coagulation or

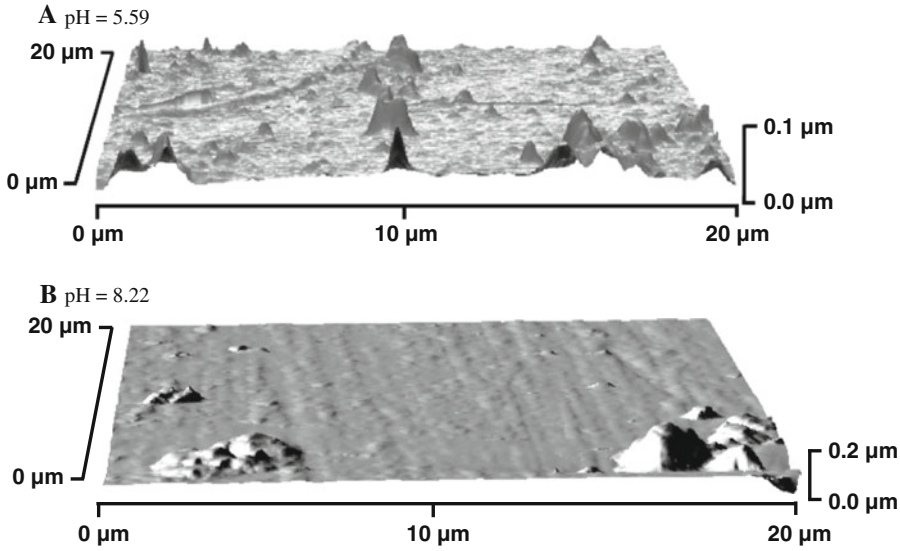

Fig. 4 Atomic force microscopy scans of filtered lake water at (**a**) acid and (**b**) alkaline pH. The scans represent the materials in three (x, y, z) dimensions. Note that the z-axis (height) differs between the two treatments

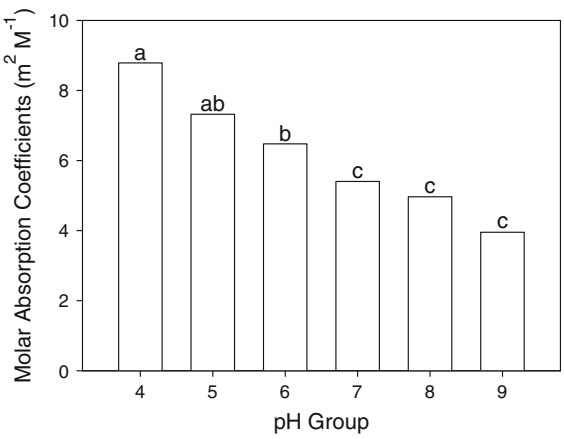

Fig. 5 Relationship between molar absorption coefficients at 440 nm and pH for surveys of lakes in northern Michigan (USA) and Quebec (Canada). Molar absorption coefficients derived from mean values of *a440* and DOC. pH groups were binned by full pH units (e.g. 4–4.99; 5–5.99; etc.) with *X*-axis labels representing the minimum value of each group. Means for each bin are presented. Letters above bars indicate differences among means ($p < 0.05$)

photomineralization. In the case of losses due to coagulation, divalent cations can suppress the solubility of the higher molecular weight humic substances inducing flocculation of these compounds (Otsuki and Wetzel 1973; Aiken and Malcolm 1987; Chin et al. 1998). For our experiments selective coagulation of a fraction of the CDOM does not account for the changes in the absorption capacity and photobleaching vulnerability of the remaining pool. We did not observe a decrease in initial DOC concentrations related to pH suggesting little or no coagulation and loss (see initial DOC values, Table 1). After the sunlight incubations, we detected only subtle DOC losses (final DOC values in Table 1). These losses were most likely due to photomineralization and were independent of the pH gradient.

We propose that the key process causing change in DOM optical properties with pH are shifts in the structural conformation of at least a portion of the pool. At low pH, DOM polymers and colloids are condensed with tight packing limiting the exposure of chromophores to light (Fig. 6). At higher (more alkaline) pH, polymers and colloids expand exposing chromophores to light (Fig. 6). This change in configuration is likely promoted by divalent cations like Ca and Mg in a manner similar to that for marine aggregates where polyanionic gels are stabilized by cations and disrupted with the addition of chelators (Chin et al. 1998). Humic acids in soils and water also change configuration in relation to shifts in pH, ionic strength of the medium, and complexing cations as measured in experimental studies using various imaging methods (Myneni et al. 1999; Baalousha et al. 2006). In our study DLS, SEM, and AFM all reveal changes in the size composition consistent with Fig. 6. It is also possible that the primary mechanism for the shift is not so much a change in pH (H^+ concentration) but a change in base cation concentration which promotes expansion and stabilization in a manner similar to marine gels (Chin et al.

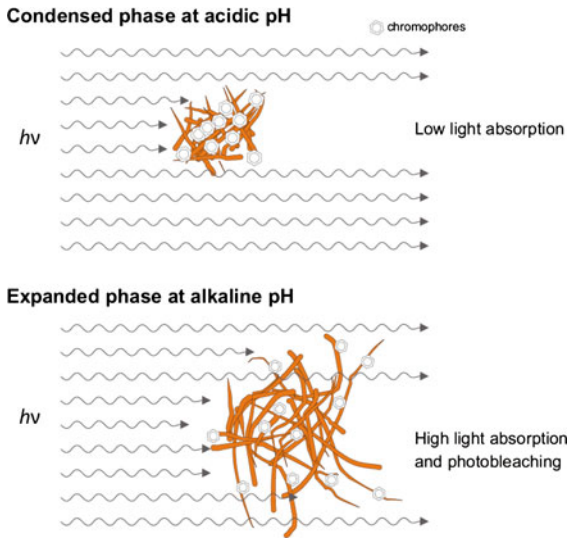

Fig. 6 Conceptual diagram illustrating contrasting states of condensation and expansion of organic matter under acidic and alkaline conditions, respectively. Under acidic conditions (*upper panel*), organic matter polymers and colloids are tightly packed and absorb relatively little light; under alkaline conditions (*lower panel*) the organic matter complexes expand resulting in greater initial light absorption and more rapid light-mediated transformations

1998). In our experiments we increased the concentration of Na^{+}. In the comparative lake studies Ca^{+2}, Mg^{+2}, K^{+}, and Na^{+} all likely increase in concentration from acidic to alkaline lakes and collectively these cations may influence DOM configuration and light absorption. Further work is needed to distinguish the relative importance of cations and hydrogen ion in determining DOM configuration, light absorption and susceptibility to photobleaching.

The finding of a strong influence of pH on DOC molar absorption of light, photobleaching, and the size of colloidal DOM has implications for inland water ecosystems undergoing environmental change. In several regions the pH of freshwater is increasing in response to decreasing inputs of acidifying pollutants. In these same regions DOC is also increasing (De Wit et al. 2007; Monteith et al. 2007). Our work indicates that the optical character of DOM is subject to change under conditions of increasing pH with greater absorption of light in fresh material and faster losses of light absorption capacity upon light exposure. On balance the molar absorption of DOC should decline as pH increases as our two lake surveys indicate. While there are a number of aquatic studies that document long term changes in pH and DOC, these studies typically do not have data on *a440* or a similar optical measurement in order to test for temporal changes in molar absorption coefficients.

The shift in photobleaching rates among lake with differing pH suggests a threshold response (Fig. 1). Molot et al. (2005) observed minimum photobleaching (absorbance loss at 300 nm) at pH 7 which is consistent with a threshold in these rates across pH gradients. DOM absorbance declines with light exposure because as photons are absorbed photochemical reactions alter chromophores. Photochemical interactions of DOM with iron and reactive oxygen species like hydroxyl radicals are important and vary with pH (Zepp et al. 1992; Molot et al. 2005). Thus, photochemical reactions may interact with the changes in structural confirmation proposed here to influence photobleaching and perhaps photooxidation. The latter process appears highest under acidic conditions (Molot et al. 2005) while photobleaching is highest under alkaline conditions as illustrated by this study. Further tests for threshold changes in photobleaching and photooxidation of DOM in relation to pH are warranted.

From an ecosystem perspective the photolability and relative transparency of DOM may strongly influence carbon cycling and the balance of autotrophy and heterotrophy. As acidity declines, DOM appears to be less susceptible to photooxidation (Molot et al. 2005) and may undergo greater photobleaching (Fig. 1). These changes due to photoprocesses also result in the provision of organic substrates to bacteria (Lindell et al. 1995; Wetzel et al. 1995). Shifts in pH could lead to greater heterotrophic bacterial production and respiration assuming continuous inputs of DOC. Increased transparency will also increase light availability for autotrophs and alter thermal structure by lowering thermocline depth. Regulation of benthic primary production indirectly by DOC via control on transparency is important in determining secondary production in nutrient-poor lakes (Karlsson et al. 2009). Rivers also vary in transparency due to CDOM, and we hypothesize this variation is partly related to acidity and cation concentrations. Finally, climate change is forecast to lead to greater DOC inputs to lakes and rivers at least in some regions of the world and as a consequence the importance of inland water in carbon processing could increase (Tranvik and

Jansson 2002; Cole et al. 2007; Tranvik et al. 2009). Our study indicates that the chemical conditions of inland waters in terms of acidity and related variables such as cation concentrations will affect how higher DOC inputs alter inland aquatic ecosystems.

Acknowledgements We thank D. Thomas, S. Scanga, M. Van de Bogert, and J Coloso for help in the lab and field. E. Urea helped with microscopy, and F. Perfectti helped with the conceptual figure. Comments by two anonymous reviewers improved the final version of this paper. Our research was supported by grants from the National Science Foundation, USA (DEB0716869, DEB0715054), Spanish Ministry of Science and Technology (DISPAR, CGL2005-000076, MAT 2009-14234-C03-02), Andalusian Research Ministry (Excellence Project FQM230-2009), and the National Research Council of Canada.

References

Aiken GR, Malcolm RL (1987) Molecular weight of aquatic fulvic acids by vapor pressure osmometry. Geochim Cosmochim Acta 51:2177–2184

Baalousha M, Motelica-Heino M, Coustumer PL (2006) Conformation and size of humic substances: effects of major cation concentration and type, pH, salinity, and residence time. Colloids Surface A Physicochem Eng Aspects 272:48–55

Bricaud A, Morel A, Prieur L (1981) Absorption by dissolved organic-matter of the sea (yellow substance) in the UV and visible domains. Limnol Oceanogr 26:43–53

Carignan R, Perceval O, Prairie YT, Parkes A. (2007) Développement d'un outil de prévention de l'eutrophisation des lacs des Laurentides et de L'Estrie. Report to the Ministère du Développement durable et des Parcs

Chin W-C, Orellana MC, Verdugo P (1998) Spontaneous assembly of marine dissolved organic matter into polymer gels. Nature 391:568–572

Cole JJ, Prairie YT, Caraco NF, McDowell WH, Tranvik LJ, Striegl RG, Duarte CM, Kortelainen P, Downing JA, Middelburg JJ, Melack J (2007) Plumbing the global carbon cycle: integrating inland waters into the terrestrial carbon budget. Ecosystems 10:171–184

Cuthbert D, del Giorgio P (1992) Toward a standard method of measuring color in freshwater. Limnol Oceanogr 37:1319–1326

de Vincente I, Ortega-Reuerta E, Romera O, Morales-Baquero R, Reche I (2009) Contribution of transparent exopolymer particles to carbon sinking flux in an oligotrophic reservoir. Biogeochemistry. doi:10:1007/s10533-009-9342-8

De Wit HA, Mulder J, Hindar A, Hole L (2007) Long-term increase in dissolved organic carbon in streamwaters in Norway in response to reduced acid deposition. Environ Sci Technol 41:7706–7713

Del Vecchio R, Blough NV (2002) Photobleaching of chromophoric dissolved organic matter in natural waters: kinetics and modeling. Mar Chem 78:231–253

Findlay S, McDowell WH, Fischer D, Pace ML, Caraco N, Kaushal SS, Weathers KC (2010) Total carbon analysis may overestimate organic carbon content of fresh waters in the presence of high dissolved inorganic carbon. Limnol Oceanogr Methods 8:196–201

Friskin BJ (2001) Revisiting the method of cumulants for the analysis of dynamic light-scatter data. Appl Optics 40:4087–4091

Karlsson J, Bystrom P, Ask J, Ask P, Persson L, Jansson M (2009) Light limitation of nutrient poor lake ecosystems. Nature 460:506–509

Kelton N, Molot LA, Dillon PJ (2007) Spectrofluorometric properties of dissolved organic matter from central and southern Ontario streams. Water Res 41:638–646

Kirk JTO (1994) Light and photosynthesis in aquatic ecosystems. Cambridge University Press, Cambridge

Koppel DE (1972) Analysis of macromolecular polydispersity in intensity correlation spectroscopy: the method of cumulants. J Chem Phys 57:4814–4820. doi:10.1063/1.1678153

Lindell MJ, Graneli W, Tranvik LJ (1995) Enhanced bacterial growth in response to photochemical transformation of dissolved organic matter. Limnol Oceanogr 40:195–199

McKnight DM, Boyer EW, Westerhoff PK, Doran PT, Kulbe T, Andersen DT (2001) Spectrofluorometric characterization of dissolved organic matter for indication of precursor organic material and aromaticity. Limnol Oceanogr 46:38–48

Miller WL (1998) Effects of UV radiation on aquatic humus: photochemical principles and experimental considerations. In: Hessen DO, Tranvik LJ (eds) Aquatic humic substances: ecology and biogeochemistry. Springer-Verlag, New York

Molot LA, Dillon PJ (1997) Photolytic regulation of dissolved organic carbon in northern lakes. Global Biogeochem Cycle 11:357–365

Molot LA, Hudson JJ, Dillon PJ, Miller SA (2005) Effect of pH on photo-oxidation of dissolved organic carbon by hydroxyl radicals in a coloured softwater stream. Aquat Sci 67:189–195

Monteith DT et al (2007) Dissolved organic carbon trends resulting from changes in atmospheric deposition chemistry. Nature 450:537–539

Morris DP, Hargreaves BR (1997) The role of photochemical degradation of dissolved organic carbon in regulating the UV transparency of three lakes on the Pocono Plateau. Limnol Oceanogr 42:239–249

Morris DP, Zagarese H, Williamson CE, Balseiro EG, Hargreaves BR, Modenutti B, Moeller R, Queimalinos XX (1995) The attenuation of solar UV radiation in lakes and the role of dissolved organic carbon. Limnol Oceanogr 40:1381–1391

Myneni SCB, Brown JT, Martinez GA, Meyer-Ilse W (1999) Imaging of humic substance macromolecular structures in water and soils. Science 286:1335–1337

Osburne CL, Zagarese HE, Morris DP, Hargreaves BR, Cravero WE (2001) Calculation of spectral weighting functions for the solar photobleaching of chromophoric dissolved organic matter in temperate lakes. Limnol Oceanogr 46:1455–1467

Otsuki A, Wetzel RG (1973) Interaction of yellow organic acids with calcium carbonate in freshwater. Limnol Oceanogr 18:490–493

Pace ML, Cole JJ (2002) Synchronous variation of dissolved organic carbon in lakes. Limnol Oceanogr 47:333–342

Prairie YT (2008) Carbocentric limnology: looking back, looking forward. Can J Fish Aquat Sci 65:54–548

Reche I, Pace ML, Cole JJ (1998) Interactions of photobleaching and inorganic nutrients in determining bacterial growth on colored dissolved organic carbon. Microb Ecol 36:270–280

Reche I, Pace ML, Cole JJ (1999) Relationship of trophic and chemical conditions to photobleaching of dissolved organic matter in lake ecosystems. Biogeochemistry 44: 259–280

Reche I, Pulido-Villena E, Conde-Porcuna JM, Carrillo P (2001) Photoreactivity of dissolved organic matter from high-mountain lakes of Sierra Nevada, Spain. Arct Antarct Alp Res 33:426–434

Santschi PH, Balnois E, Wilkinson K, Zhang J, Buffle J, Guo L (1998) Fibrillar polysaccharides in marine macromolecular organic matter, as imaged by atomic force microscopy and transmission electron microscopy. Limnol Oceanogr 43:896–908

Tranvik LJ, Jansson M (2002) Climate change—export of organic carbon. Nature 415:861–862

Tranvik LJ et al (2009) Lakes and reservoirs as regulators of carbon cycling and climate. Limnol Oceanogr 54:2298–2314

Tzortziou M, Osburn CL, Neale PJ (2007) Photobleaching of dissolved organic material from tidal marsh-estuarine system of the Chesapeake Bay. Photochem Photobiol 83:782–792

Verdugo P, Alldredge AL, Azam F, Kirchman DL, Passow U, Santschi PH (2004) The oceanic gel phase: a bridge in the DOM-POM continuum. Mar Chem 92:67–85

von Wachenfeldt E, Tranvik LJ (2008) Sedimentation in boreal lakes—the role of flocculation of allochthonous dissolved organic matter in the water column. Ecosystems 11: 803–814

Wetzel RG (2001) Limnology: lake and river ecosystems. Academic Press, Burlington

Wetzel RG, Hatcher PG, Bianchi TS (1995) Natural photolysis by ultraviolet irradiance of recalcitrant dissolved organic matter to simple substrates for rapid bacterial metabolism. Limnol Oceanogr 40:1369–1380

Williamson CE, Morris DP, Pace ML, Olson OG (1999) Dissolved organic carbon and nutrients as regulators of lake ecosystems: resurrection of a more integrated paradigm. Limnol Oceanogr 44:795–803

Wilson HF, Xenopoulos MA (2009) Effects of agricultural land use on the composition of fluvial dissolved organic matter. Nat Geosci 2:37–41

Zepp RG, Faust BC, Hoigné J (1992) Hydroxyl radical formation in aqueous reactions (pH 3–8) of iron (II) with hydrogen-peroxide: the photo-Fenton reaction. Environ Sci Technol 26:313–319